# $SrFeO_{2.95}$: A helical antiferromagnet with large magnetoresistance

Y. M. Zhao*
*Department of Physics, Shantou University, Shantou 515063, Guangdong, China, and Laboratoire CRISMAT, UMR 6508 associée au CNRS, ISMRA et Université de Caen 6, Boulevard du Maréchal Juin, 14050 CAEN Cedex, France*

R. Mahendiran, N. Nguyen, and B. Raveau
*Laboratoire CRISMAT, UMR 6508 associée au CNRS, ISMRA et Université de Caen 6, Boulevard du Maréchal Juin, 14050 CAEN Cedex, France*

R. H. Yao
*Department of Physics, Shantou University, Shantou 515063, Guangdong, China*
(Received 17 April 2000; revised manuscript received 10 January 2001; published 20 June 2001)

Resistivity, magnetoresistance, and Mössbauer effect of metallic spiral antiferromagnet $SrFeO_{2.95}$ have been examined in the temperature range 4.5–300 K. A large negative magnetoresistance below 50 K is observed. We find hysteresis in resistivity in 0 and 9 T due to the coexistence of antiferromagnetic and paramagnetic domains in the temperature region 50–80 K. Our result shows two contributions to magnetoresistance: one below 50 K that is due to helical-conical spin transformation and another close to $T_N$ that is due to reduced spin fluctuation under magnetic field.

DOI: 10.1103/PhysRevB.64.024414 PACS number(s): 75.50.Ee, 75.90.+w

Colossal magnetoresistance (CMR)—a huge decrease in resistance in response to a magnetic field—has recently been observed in manganese oxide with perovskite structure. This effect has attracted considerable interest from both fundamental and practical points of view.[1] But the criteria for achieving (and hence optimizing) CMR is not clear, presenting a challenge for materials scientists. The accepted description of ferromagnetic and metallic behavior in the manganite perovskite invokes the ''double-exchange'' mechanism, whereby ferromagnetic coupling between localized Mn $t_{2g}^3$ spins is mediated by the hopping of $e_g$ electrons.[2] Furthermore, recent theoretical and experimental evidence indicates that the important feature of the manganites is the competition between double-exchange ferromagnetism and another instability associated with electron-lattice coupling, partially the Jahn–Teller-type, leading to (JT) polaron formation.[3,4] Most recently, Uehara *et al.*[5] have shown that the instability relevant for colossal magnetoresistance is a static charge-ordered (CO) state with a particular modulation, resulting in the large-scale coexistence of this CO phase with a ferromagnetic (FM) metallic phase. Large magnetoresistance has also been found in $Ln_{1-x}A_xCoO_{3-\delta}$, where Ln=Y or La and $A$=Pb, Ca, Sr, or Ba.[6] The magnetoresistance of the Co-containing samples increases as the size of the alkaline earth ions increase, in sharp contrast with Mn-containing compounds, in which the magnetoresistance effect increases as the size of the alkaline earth ion decreases. The question arises whether these effect are unique to Mn- and Co-based perovskite oxides or can be found in other Fe-based perovskite materials.

The Fe(IV) perovskite $SrFeO_3$ has long been known as a conducting antiferromagnet with a magnetic transition temperature of 134 K and resistivity of about $10^{-3}\,\Omega$ cm.[7,8] It has a proper screw spin structure with the propagation vector parallel to a [111] direction and does not show a cooperative Jahn–Teller distortion down to 4.2 K.[9] The absence of Jahn–Teller distortion in this high spin $3d^4$ state was explained by high electrical conductivity where the $e_g^*$ orbitals are broadened into an itinerant electronic conduction band. The low electron density at the iron nucleus observed by the Mössbauer spectroscopy,[7] as well as molecular orbital calculation and analysis of photoelectron spectra, which is also evidence that $Fe^{4+}$ is in a high-spin state, elucidate a strong covalency in $SrFeO_3$. On the other hand, for oxygen deficient compounds of $SrFeO_{3-\delta}$, the Nèel temperature decreases from 134 K for $\delta=0$ to 80 K for $\delta=0.16$ and the electrical conductivity changes with increasing $\delta$ from metallic to semiconducting with an activation energy increasing up to 0.08 eV for $\delta=0.16$.[10] Although this particular compound has been well studied by Mössbauer spectroscopy, magnetization, and neutron diffraction techniques[7,8,10] with unfortunately, several contradictions still subsist, leading to confusion regarding the nature of the $3d$ electron. These conflicting results may be traced back to the great sensitivity of the magnetic properties to the oxygen substoichiometry. There is, to our knowledge, no data reported on magnetoresistance of Fe-based perovskites. Here we report the existence of a large magnetoresistance effect in the Fe-based perovskites $SrFeO_{2.95}$—that does not possess distortion-inducing ions such as manganese or cobalt. The realization of CMR in Fe-based compounds having the perovskite structure should open up a vast range of materials for the further exploration and exploitation of this effect.

Polycrystalline samples of $SrFeO_{3-\delta}$ were synthesized by direct solid state reaction of $SrCO_3$ and $Fe_2O_3$, mixed in stoichiometric molar proportions. The preparation will be described in greater detail elsewhere.[11] Analysis for available oxygen using redox titration which led to the composition $SrFeO_{2.95}$. The oxygen deficiency $\delta \leqslant 0.05$ is consistent with the data of the composition dependence of the Néel tempera-

 

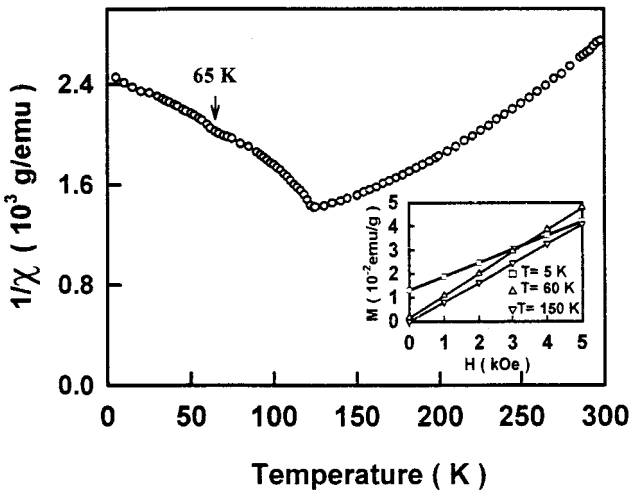


FIG. 1. Inverse ac susceptibility of $SrFeO_{2.95}$ measured in 3 G as a function of temperature. Inset: magnetization of $SrFeO_{2.95}$ as a function of field at several temperatures.

ture obtained by MacChesney *et al.*[10] The resistivity of samples as a function of magnetic field (perpendicular to the probing current) and temperature was measured by the four-probe method, using physical properties measurement system (PPMS) with a superconducting 9-T magnet. Magnetic properties were measured using dc and ac SQUID system with the maximum magnetic field of 5 T. Mössbauer absorption powder spectra were recorded at various temperatures using a conventional spectrometer with a $^{57}Co/Rh$ source. Isomer shift values are quoted relative to metallic $\alpha$-Fe at 293 K. Powder x-ray diffraction analysis showed that the produced samples are single phase, and the crystal structure at room temperature exhibits cubic perovskite symmetry with lattice constant $a=3.852$ Å. Electron microscopy spectra showed that the underlying sample is absolutely homogeneous with a very weak oxygen deficient ordering.

Figure 1 shows the temperature dependence of the inverse susceptibility ($\chi^{-1}$). The minimum in $\chi^{-1}$ at 107 K is associated with the onset of helical antiferromagnetism.[9] We find a strong deviation of $\chi^{-1}(T)$ from Curie–Weiss law in the temperature range between 107–200 K. This deviation from Curie–Weiss law can be caused by the presence of ferromagnetic clusters in the paramagnetic phase or by spin fluctuation effects. If it is due to the ferromagnetic clusters, the field dependence of magnetization ($M$) should show a nonlinear increase with magnetic field $H$, but we see a linear $M(H)$ behavior up to 5 T as show in the 150 K data inset of Fig. 1. Hence, the observed deviation from Curie–Weiss law is caused by spin fluctuation effect. We also see a weak feature in $\chi^{-1}$ at 65 K whose origin is will be clear after presenting the Mössbauer result. $M$ at low temperature shows a rapid increase at low fields (see 5 K data in the inset of Fig. 1) and increases without saturation up to 5 T. The low field rise of $M$ is also seen in helical antiferromagnets MnSi (Ref. 12) and is caused by domain rotation.

Figure 2 shows the Mössbauer spectra at different temperatures. The main six lines pattern at 4.5 K is due to the magnetic $Fe^{4+}$ ion in high-spin localized state ($H_f=32.6$ T) and the small sextet with $H_f=43.5$ T corresponds to the magnetic $Fe^{3+}$ ion, while the raw data in these figures are shown by dots, computer generated curves are shown by lines. The relative intensity of these $Fe^{3+}$ and $Fe^{4+}$ sites confirms the oxygen content $O_{2.95}$. At 50 K, the magnetic sextet of $Fe^{4+}$ site is also evidenced, but the small contribution of $Fe^{3+}$ is nonobservable. On the spectrum at 80 K, in addition to magnetic $Fe^{4+}$ site, we see a contribution of paramagnetic $Fe^{3+\delta}$ ion. Its isomer shift value (IS=0.13 mm/s) is intermediate between those generally expected for high-spin localized $Fe^{3+}$ and $Fe^{4+}$. An estimate of the relative number of magnetic $Fe^{4+}$ to paramagnetic $Fe^{3+\delta}$ by comparing the area under the absorption peaks gave a good agreement with that using the peak values of absorption, which may more readily be affected by line broadening. The estimate gave, for example, 72% of magnetic $Fe^{4+}$ site and 28% of paramagnetic $Fe^{3+\delta}$ ion. At 293 K, besides the $Fe^{4+}$ component which is paramagnetic, we observe also this intermediate valence $Fe^{3+\delta}$ site with the same IS and intensity values at 80 K. Table I summarizes our Mössbauer data. In order to show clearly the origin of the weak feature in $\chi^{-1}$

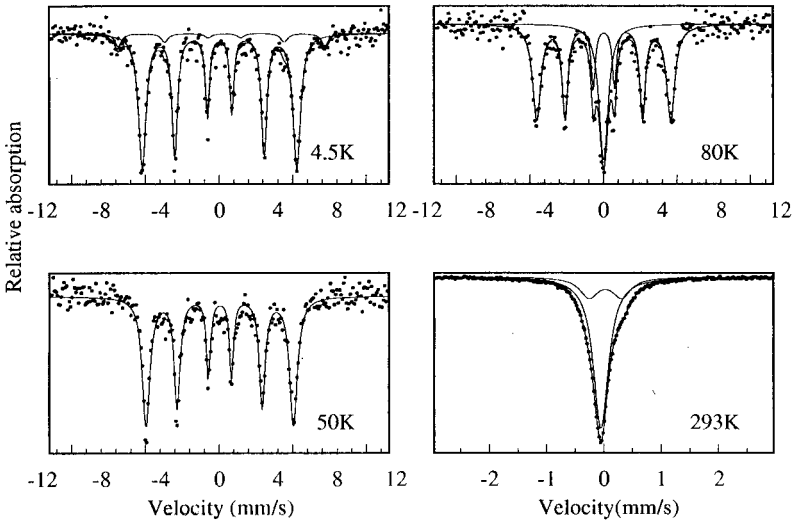


FIG. 2. Mössbauer spectra of $SrFeO_{2.95}$ as a function of temperature.

TABLE I. Isomer shift (IS), quadrupole shift ($2\varepsilon$), quadrupole splitting (QS), hyperfine field ($H_f$), and relative intensity (%) of iron site observed in $^{57}$Fe Mössbauer spectra of $SrFeO_{3-\delta}$ at 4.5, 50, 60, 65, 70, 80, and 293 K, respectively.

| $T$ (K) | Iron site | IS ($\pm$0.02 mm/s) | $2\varepsilon$ $\pm$0.02 mm/s or QS ($\pm$0.02 mm/s) for paramagnetic site | $H_f$ ($\pm$0.1 T) | % ($\pm$5) |
|---|---|---|---|---|---|
| 4.5 | $Fe^{4+}$ | 0.16 | 0 | 32.6 | 92 |
| | $Fe^{3+}$ | 0.39 | $-0.20$ | 43.5 | 8 |
| 50 | $Fe^{4+}$ | 0.16 | 0 | 31.1 | 100 |
| 60 | $Fe^{4+}$ | 0.16 | 0 | 30.8 | 100 |
| 65 | $Fe^{4+}$ | 0.16 | 0 | 30.2 | 100 |
| 70 | $Fe^{4+}$ | 0.15 | 0 | 29.6 | 88 |
| | $Fe^{3+\delta}$ | 0.13 | 0 | Paramagnetic | 12 |
| 80 | $Fe^{4+}$ | 0.14 | 0 | 28.3 | 72 |
| | $Fe^{3+\delta}$ | 0.13 | 0 | Paramagnetic | 28 |
| 293 | $Fe^{4+}$ | 0.06 | 0 | Paramagnetic | 76 |
| | $Fe^{3+\delta}$ | 0.13 | 0.57 | Paramagnetic | 24 |

around 65 K, we performed more precise Mössbauer experiments in this critical temperature region. The peaks (not show here) assigned to paramagnetic $Fe^{3+\delta}$ on the spectrum at 80 K are considerably broader and weaker but definitely identifiable at 70 K. They decrease with decrease temperatures and disappear around 65 K. While the hyperfine fields associated with magnetic $Fe^{4+}$ peaks, as shown in Table I, show smooth decrease in the value on cooling around 65 K. The change of isomer shift at this temperature region is relatively small (Table I). The slight fluctuation of hyperfine field (see the data in Table I) between 50–80 K does not allow clearly to see any abrupt change of the angle between the magnetic moment of neighboring $t_{2g}$ spins in this helical magnet with noncolinear spin configuration around 65 K. The Mössbauer analysis results and the oxygen content $O_{2.95}$ lead to $\delta=0.6$.

Figure 3 shows the resistivity ($\rho$) under $H=0$ and 9 T on left-hand scale and magnetoresistance [$MR=(\rho(H)-\rho(0))/\rho(0)$] on the right-hand scale. $\rho(0)$ shows metallic-like behavior ($d\rho/dT>0$) in the temperature range 300–107 K, a rapid decrease just below $T_N$ and finally an upturn occuring around 25 K while cooling. We find hysteresis in $\rho$ in the temperature range over 25–80 K between cooling and warming. A large decrease in resistivity under 9 T occurs below 50 K. As $T$ increases MR decreases nearly to zero in between 90–100 K and show a small peak around $T_N=104\,\mathrm{K}(<T_N=107\,\mathrm{K})$. Small negative MR is also found up to 300 K. Figure 4 shows the field dependence of MR. At 20 K MR remains constant ($MR=0$) up to $H=3.8$ T and shows smooth increase in the value as $H$ increases further. The value of MR at 9 T is 12%, slightly lower than the value got from isofield temperature scan in Fig. 3. As $H$ is reduced to 0 T, we find MR remains nearly unchanged as seen in $La_{1-x}Sr_xCoO_3(x<0.07)$.[13] The hysteresis in MR decreases with increasing temperature, and we find MR is quadratic with $H$ at 150 K, in the spin fluctuation region above $T_N$.

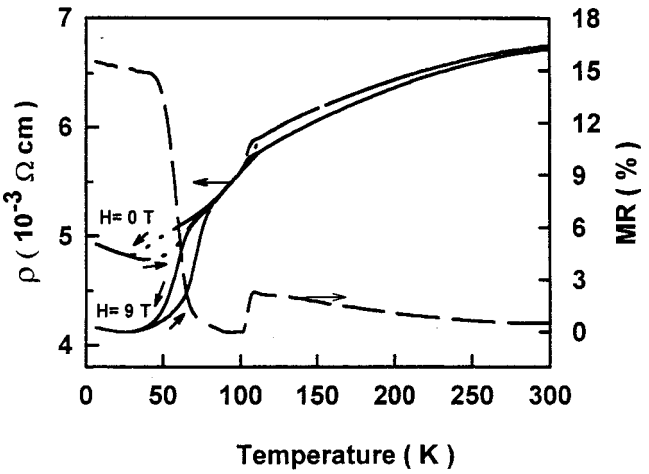


FIG. 3. Temperature dependence of resistivity $\rho(T)$ in applied field of 0 and 9 T for $SrFeO_{2.95}$. Also shown is the MR [$MR=(\rho(0)-\rho(9\,\mathrm{T}))/\rho(0)\times100$].

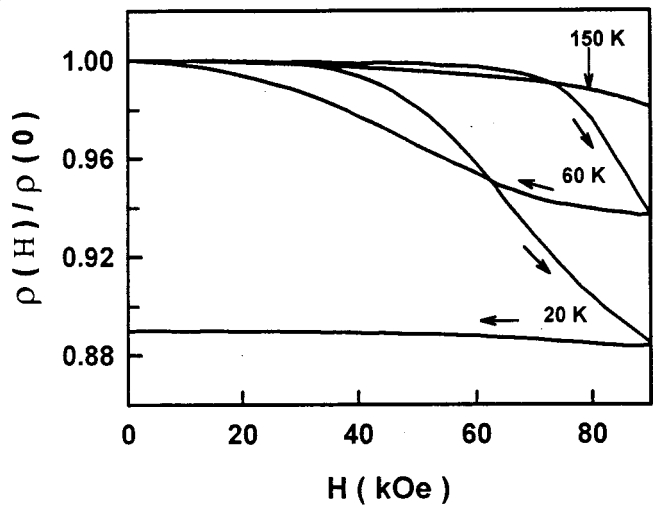


FIG. 4. Resistivity, normalized to the value at $H=0$, versus field for $SrFeO_{2.95}$ at several temperatures.

Now we try to understand the observed electrical and magnetic transport behaviors. The observed thermal evolution of $\rho(0\,T)$ is closely connected with the subtle variation in $Fe^{4+}/Fe^{3+}$ ratio and magnetic nature of these ions as found in Mössbauer study. The null quadrupolar electric interactions of $Fe^{4+}$ ions from 300 K down to 4 K suggests that $(Fe^{4+}O_6)^{8-}$ octahedra are not statically distorted. However, paramagnetic domains consisting mainly of $Fe^{3+\delta}$ ions with isomer shift IS$=0.13$ mm/s and relative intensity of about 25% remains down to 70 K and disappear at 65 K as our Mössbauer results show in Table I. This $Fe^{3+\delta}$ electronic configuration is due to the electron delocalization between $Fe^{3+}$ and $Fe^{4+}$. The Mössbauer data between 80 and 50 K clearly show that these paramagnetic domains vanish around 65 K, and thus the weak feature around this temperature is connected with the disappearance of $Fe^{3+\delta}$ paramagnetic domains when the temperature decreases ($T<65$ K). Electrical conduction in $SrFeO_3$ mainly occurs in the $\sigma^*$ narrow band of $e_g$ parentage while $t_{2g}^3$ electrons in $\pi^*$ band are localized. At 300 K, $e_g$ electrons in $\sigma^*$ band are itinerant as suggested by the low value of resistivity ($\rho_{300}=6.7\times10^{-3}\,\Omega$ cm) and Mössbauer data. As $T$ lowers to $T_N=107$ K, interatomic Hund's coupling polarizes the $\sigma^*$ conduction band. Ferromagnetic spin alignment of $e_g$ electrons in the $\sigma^*$ band enhances carrier mobility and hence $\rho$ decreases rapidly just below $T_N=107$ K. Hund's coupling can also ferromagnetically align the localized $t_{2g}^3$ spins at each Fe sites, but antiferromagnetic $t_{2g}^3$-$O$:$2P_\pi$-$t_{2g}^3$ superexchange interaction competes with it. The results is the helical spin structure with near-neighbor ferromagnetic coupling and next nearest-neighbor antiferromagnetic coupling.[9,14,15] Oda *et al.*[15] shown that the angle between the magnetic moments of nearest-neighboring Fe ions increase from 42° at $T_N$ to 47° at 4.2 K in $SrFeO_{2.90}$. The propagation vector $Q$ was also found to show smooth increase from $0.118a^*$ at $T_N$ to a constant $0.130a^*$ ($a^*=2\pi/a_0$) below 50 K.[15] It is likely that such changes in $Q$, equivalent to bond angle between the nearest Fe moments, also occur in our sample below 50 K as suggested by a sudden change in magnetoresistance above 50 K that we will see later. Our analysis of the resistivity data interms of known mechanisms is complicated by the fact that different samples from the same batch (prepared under same conditions) showed different temperature dependence of $\rho$, particularly nonlinear $\rho(T)$ behavior above $T_N$ and magnitude of the resistivity drop below $T_N$. This observation, perhaps, reflects the differences in oxygen vacancies distribution. However, all our samples showed metalliclike ($d\rho/dT>0$) resistivity behavior above $T_N$, hysteresis in $\rho$ over certain temperature range below $T_N$ and a resistivity minimum below 50 K. A low temperature resistivity minimum is found in several metallic oxides[16] whose origin vary from electron-electron ($e$-$e$) interaction, weak localization effects to spin-state transition.[17] Our resistivity data at low temperature, below the resistivity minimum can be fitted nicely to $\rho=\rho_0-mT^{1/2}$ for different values of applied magnetic field as shown in Fig. 5. The first term $\rho_0=\rho_{imp}+\rho_{mag}$ contains contribution from impurity scattering ($\rho_{imp}$) and magnetic scattering ($\rho_{mag}$). The second term $mT^{1/2}$ is due to electron-electron interactions. Our fit shown in Fig. 5 suggests that while $e$-$e$ interaction is not affected by magnetic field, a large decrease in $\rho_0$ occurs. Such a change in $\rho_0$ is caused by decrease in $\rho_{mag}$ with increased $H$. In a helical magnet, spin configurations can influence $\rho_{mag}$ by changing from helical to conical, conical to fan and finally to ferromagnetic alignment as the field increases.[12] Our magnetization data (in the inset of Fig. 1) at 5 K suggest that ferromagnetism is not achieved even at 5 T. The linear increase of $M$ is possibly connected with the transition from helical to conical. The change of spin structure with $H$ reduces the scattering of $e_g$-electron, causing the observed negative magnetoresistance. Similar behavior of MR is also observed in metallic helical antiferromagnet MnSi.[12] The observed hysteresis in MR while reducing $H$ from the highest value suggests very slow relaxation of spins from conical to helical magnetic structure. Such hysteresis in MR was also seen in $La_{1-x}Sr_xCoO_3$($x<0.07$),[13] $Nd_{0.5}Ca_{0.5}MnO_{3-\delta}$,[14] and recently it has been confirmed by magnetization measurement[18,19] that slow lattice relaxation also accompanies spin relaxation. It is likely that similar magnetic elastic relaxation effects are present in our sample. As $T$ increase above 40 K, contribution of MR from helical to conical transformation of spin also decreases repidly for two different reasons: under $H=0$ T, there is a variation in angle between the mements of nearest-neighbor Fe ions above 50 K;[12] also, paramagnetic $Fe^{3+\delta}$ domains intervene the magnetic ordering. These changes in zero field consequently affect the value of magnetoresistance which decrease from 15% at 50 K to nearly zero at 100 K. As $T$ approaches to $T_N$, a new contribution to MR occurs. This contribution which peaks around $T_N$ is caused by the partial suppression of spin fluctuation as seen in MnSi.[12]

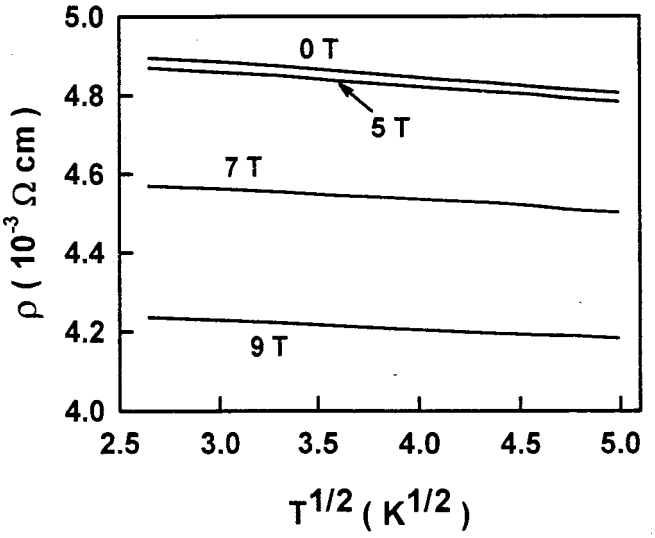


FIG. 5. Resistivity vs $T^{1/2}$ in magnetic field between 0 and 9 T, as labeled, for $SrFeO_{2.95}$.

In conclusion, we have studied the resistivity, magnetoresistance, and Mössbauer effect in metallic spinel antiferromagnetic $SrFeO_{2.95}$ in the temperature range from 4.5–300

K. We have found hysteresis of resistivity in 0 T as well as 9 T due to the coexistence of antiferromagnetic and paramagnetic domains. We conclude that there are two contributions to magnetoresistance, one below 50 K, due to helical-conical spin transformation, and another near $T_N$ due to reduced spin fluctuation.

This project was funded in part by K. C. Wong, Y. D. Huo, and NSFC Grant supported through C. N. R. S. and E. C. China, respectively. Y.M.Z. acknowledges with pleasure the assistance of Laboratoire CRISMAT, ISMRA et Université de Caen, 14050 CAEN Cedex, France, in some of the syntheses and measurement.

*Author to whom correspondence should be addressed. Department of Physics, Shantou University, Shantou 515063, Guangdong, China.

[1] See, for example, *Science and Technology of Magnetic Oxides*, edited by M. F. Hundley, J. H. Nickel, R. Ramesh, and Y. Tokura, MRS Symposia Proceedings No. 494 (Materials Research Society, Pittsburgh, 1998).
[2] C. Zener, Phys. Rev. **82**, 403 (1951).
[3] A. J. Mills, P. D. Littlewood, and B. I. Shraiman, Phys. Rev. Lett. **74**, 5144 (1995); H. Roder, J. Zhang, and A. R. Bishop, *ibid.* **76**, 1356 (1996).
[4] J-S. Zhou, and J. B. Goodenough, Phys. Rev. Lett. **80**, 2665 (1995).
[5] M. Uehara, S. Mori, C. H. Chen, and S-W. Cheong, Nature (London) **399**, 560 (1999).
[6] G. Briceno, H. Chang, X. Sun, P. G. Schultz, and X.-D. Xiang, Science **270**, 273 (1995).
[7] P. K. Gallagher, J. B. MacChesney, and D. N. E. Buchanan, J. Chem. Phys. **41**, 2429 (1964).
[8] H. Watanabe, J. Phys. Soc. Jpn. **12**, 515 (1957).
[9] T. Takeda, Y. Yamaguchi, and H. Watanabe, J. Phys. Soc. Jpn. **33**, 967 (1972).
[10] J. B. MacChesney, R. C. Sherwood, and J. F. Potter, J. Chem. Phys. **43**, 1907 (1965).
[11] Y. M. Zhao *et al.* (unpublished).
[12] K. Kadowaki, K. Okuda, and M. Date, J. Phys. Soc. Jpn. **51**, 2433 (1982).
[13] R. Mahendiran and A. K. Raychaudhuri, Phys. Rev. B **54**, 16044 (1996).
[14] J. B. Goodenough and J.-S. Zhou, Chem. Mater. **10**, 2980 (1998).
[15] H. Oda, Y. Yamaguchi, H. Takei, and H. Watanabe, J. Phys. Soc. Jpn. **42**, 101 (1977).
[16] A. K. Raychaudhuri, Adv. Phys. **44**, 21 (1995).
[17] P. A. Lee and T. V. Ramakrishnan, Rev. Mod. Phys. **57**, 287 (1985).
[18] R. Mahendiran, R. Mahesh, R. Gundakaram, A. K. Raychauhuri, and C. N. R. Rao, J. Phys.: Condens. Matter **8**, L455 (1996).
[19] R. Mahendiran *et al.* (unpublished).